Potential Profile across a Conducting Polymer Film during Mediated Electrolysis

Huanyu Mao† and Peter G. Pickup*

Department of Chemistry, Memorial University of Newfoundland, St. John's, Newfoundland, Canada A1B 3X7

Received November 25, 1991. Revised Manuscript Received February 20, 1992

Rotating disk voltammetry of ferrocene oxidation at electrodes coated with poly[1-methyl-3-(pyrrol-1-ylmethyl)pyridinium]$^+$ films of varying thickness has been used to obtain potential profiles across the polymer. The potential of the polymer increases logarithmically with distance from the polymer/solution interface, with a slope of ca. 90 mV/decade. This nonlinear relationship clearly indicates that the polymer does not behave like a metallic conductor. Instead, electron transport is driven by a linear concentration gradient of charge carriers (oxidized sites) as in a polymer with discreet redox sites. Knowledge of the potential profile across the polymer allows calculation of in situ conductivity as a function of potential. Results are in good agreement with values determined by dual electrode voltammetry.

Introduction

In most of the electrochemical applications of conducting polymers, electron transport occurs through a polymer film containing an oxidation state gradient. Since the conductivity of a conducting polymer depends on its degree of oxidation,[1] which is a function of potential, it is clear that the potential profile across the polymer will be nonlinear. Under these conditions, the conventional treatment of the polymer as an Ohmic conductor is inappropriate.[2]

The electrolytic oxidation of a solution species at a conducting polymer electrode is a practical example where the effects of an oxidation state gradient and the resulting nonlinear potential profile must be considered. The degree of oxidation of the polymer decreases toward the polymer/solution interface, resulting in an increasing potential gradient. We report here a method for determining the potential profile across the polymer film during steady-state electrolysis of a solution species. The potential profile allows us to model electron transport across the film at constant current and to obtain the in situ conductivity of the polymer as a function of potential. Potential dependent conductivities from dual electrode voltammetry are also presented for comparison.

The in situ conductivity of conducting polymers has been of much interest since it was shown in an early report on polypyrrole that this polymer was conductive when oxidized but not when reduced.[3] This phenomenon was first investigated quantitatively by Wrighton and coworkers,[4] who used a polymer-coated microelectrode array to measure the conductivity of polypyrrole as a function of potential. These measurements were performed with the polymer immersed in an electrolyte solution, which also allowed the potential profile across the polymer layer to be measured. With one side of the array at an oxidizing potential and the other at a reducing potential, a nonlinear potential profile was obtained. The steepest potential drop occurred at the low potential end of the array, consistent with the low conductivity of the reduced polymer.

Rotating disk voltammetry of a solution species at a conducting polymer-coated electrode represents a well-defined example of the general phenomenon of nonlinear potential profiles in electrochemical applications of conducting polymers.[2] The controlled mass-transport conditions at the rotating electrode allow mass transport effects to be separated from the influence of charge transport in the polymer. A solution species which does not permeate into the polymer matrix and which exchanges electrons rapidly with the polymer, simplifies the analysis, and so we use ferrocene oxidation at poly[1-methyl-3-(pyrrol-1-ylmethyl)pyridinium]$^+$ (poly-MPMP$^+$) in acetonitrile, which has been shown to satisfy these criteria.[2] A schematic diagram of the rotating disk electrode experiment and the resulting potential profile across the polymer film are shown in Figure 1A. The potential profile across the film at any particular current is obtained by measuring the potentials required to pass the same current through a series of thinner films under the same conditions.

Poly-MPMP$^+$ and other conducting polymers with cationic substituents have been attracting increasing interest because of applications in areas such as electrocatalysis,[5-7] electroanalysis,[7] and electrochromics.[8] Investigation of the conductivity of these materials provides data needed to analyze and predict their performance in these applications and furthers our understanding of the factors that determine the conductivity of polypyrroles.

Experimental Section

Electrochemistry. Electrochemical experiments were carried out in conventional three compartment glass cells under an argon atmosphere at 23 ± 2 °C. Three- or four-electrode arrangements consisting of a 0.458 cm^2 Pt rotating disk electrode sealed in PTFE (Pine Instruments) or two 1.3×10^{-4} cm^2 Pt disks sealed in glass (for dual electrode voltammetry), a Pt wire counter electrode, and a saturated sodium chloride calomel electrode (SSCE) reference electrode were used. All potentials are quoted with respect to the SSCE. Electrochemical instrumentation consisted of a Pine Instruments RDE4 potentiostat/galvanostat, a BBC MDL780 X-Y recorder, and a Pine Instruments ASR electrode rotator. All potentials measured from rotating disk voltammograms have

†Present address: Moli Energy (1990) Ltd.; 3958 Myrtle St., Burnaby, B.C. V5C 4G2, Canada.

*To whom correspondence should be addressed.

(1) Ofer, D.; Crooks, R. M.; Wrighton, M. S. *J. Am. Chem. Soc.* **1990**, *112*, 7869-7879.
(2) Mao, H.; Pickup, P. G. *J. Am. Chem. Soc.* **1990**, *112*, 1776-1782.
(3) Diaz, A. F.; Castillo, J. I. *J. Chem. Soc., Chem. Commun.* **1980**, 397-398.
(4) Kittlesen, G. P.; White, H. S.; Wrighton, M. S. *J. Am. Chem. Soc.* **1984**, *106*, 7389-7396.
(5) Pickett, C. J.; Moutet, J.-C. *J. Chem. Soc., Chem. Commun.* **1989**, 188-189.
(6) Keita, B.; Bousziz, D.; Nadjo, L.; Deronzier, A. *J. Electroanal. Chem.* **1990**, *279*, 187-203.
(7) Mao, H.; Pickup, P. G. *J. Electroanal. Chem.* **1989**, *265*, 127-142.
(8) Iyoda, T.; Alba, M.; Saika, T.; Honda, K.; Shimidzu, T. *J. Chem. Soc., Faraday. Trans.* **1991**, *87*, 1765-1769.

0897-4756/92/2804-0642$03.00/0

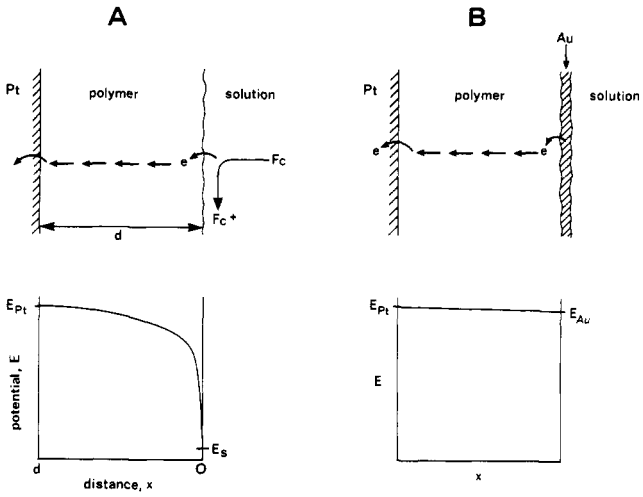

Figure 1. Schematic diagrams of the rotating disk voltammetry (A) and dual electrode voltammetry (B) experiments, and the resulting potential profiles across the polymer film. Fc is ferrocene, E_{Pt} is the potential at the polymer/electrode interface, E_s is the potential at the polymer/solution interface, and E_{Au} is the potential of the porous gold coating in dual-electrode voltammetry.

been corrected for the IR drop due to the uncompensated solution resistance (48 Ω).

Small Amplitude Dual-Electrode Voltammetry. A sandwich electrode[9] is prepared by vapor deposition of a thin porous gold film over a polymer-coated Pt disk electrode. The gold film also covers an adjacent Pt disk which allows potential control at the polymer/solution interface. With the electrode immersed in an electrolyte solution, a four-electrode potentiostat is used to maintain a small constant potential difference (10 mV) across the polymer film while its average potential is slowly scanned. The steady-state voltammogram thus obtained is converted to a conductivity vs potential plot by applying Ohm's law. A schematic diagram of the dual electrode experiment is shown in Figure 1B. The assumption of a linear potential profile when the potential difference across the polymer is small has been shown to be valid in other work.[10]

Chemicals. 1-Methyl-3-(pyrrol-1-ylmethyl)pyridinium tetrafluoroborate ($MPMPBF_4$) was prepared as previously described.[7] Ferrocene (Aldrich), tetraethylammonium tetrafluoroborate (Et_4NBF_4, Fluka), and acetonitrile (Fisher, HPLC grade) were used as received.

Preparation of Polymer Films. $MPMPBF_4$ was polymerized from 0.05 M acetonitrile solutions containing 0.1 M Et_4NBF_4 at a constant current density of 0.8 mA cm^{-2}. A charge density of 0.15 C cm^{-2} produces a 1.0-μm-thick polymer film.[7]

Results

Rotating Disk Voltammetry. Figure 2 shows rotating disk voltammograms of ferrocene at bare Pt and poly-$MPMP^+$-coated Pt electrodes. As previously discussed,[2] the displacement of the oxidation wave to higher potentials at the coated electrodes demonstrates that ferrocene does not diffuse into the polymer matrix. The increasing displacement with increasing polymer film thickness (d) shows that electron transport across the polymer is the rate-limiting process before the limiting current is reached. The limiting current is mass transport controlled and is of no interest here.

Potential Profile. The potential profile across a poly-$MPMP^+$ film, mediating the oxidation of ferrocene at a particular current density (below the limiting current), can be composed by combining data for a collection of thinner films operating under the same conditions. For

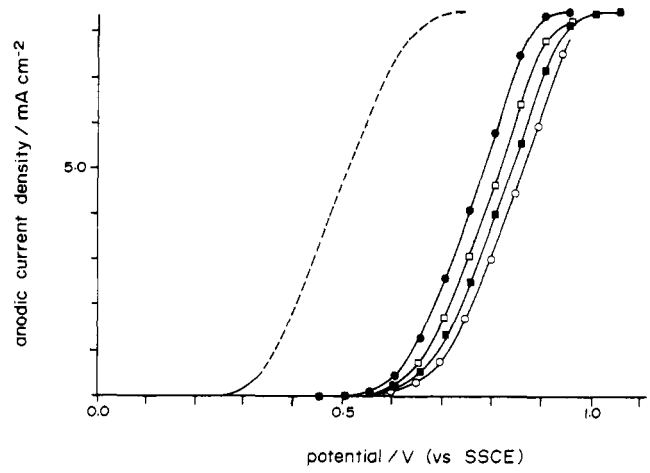

Figure 2. Rotating disk voltammograms of ferrocene (5 mM) in acetonitrile + 0.1 M Et_4NBF_4 at bare (---, 10 mV s^{-1}) and poly-$MPMP^+$-coated Pt electrodes (steady-state currents after 10–18 s at constant potential). Polymer film thickness = 1 (●), 2 (□), 4 (■), and 6 μm (○). Rotation rate = 2000 rpm.

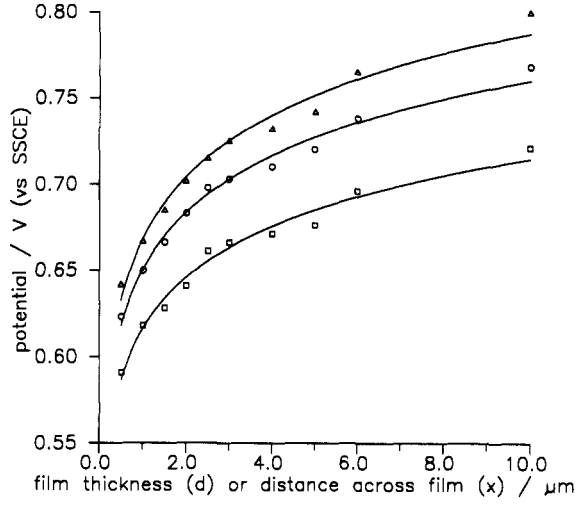

Figure 3. Plots of potential at the underlying Pt electrode (E_{Pt}) vs film thickness (d) at constant current densities of 1.1 (□), 3.3 (○), and 5.5 (Δ) mA cm^{-2}, from the rotating disk voltammograms shown in Figure 2 (and others recorded under the same conditions). The solid lines are logarithmic least-square fits. These plots also represent potential vs distance from the polymer/solution interface (x) for a 10 μm film.

example, the potential at the underlying Pt electrode (E_{Pt}) required to drive a certain current density through a 1-μm-thick film provides the potential at a plane 1 μm from the polymer/solution interface for a 2-μm film at the same current density. The reason for this is that the potential at the polymer/solution interface (E_s) is determined only by the mass transport conditions and the current, which are kept constant. The potential profile across the outer 1 μm of the 2-μm film must therefore be the same as that across the 1-μm film. The only assumptions here are that the film is homogeneous, its surface roughness is independent of film thickness, and the current is below the limiting current. Scanning electron microscopy[7] and other studies[2,11] indicate that poly-$MPMP^+$ is homogeneous and relatively smooth. Slow charge-transfer kinetics, the Donnan potential, and the uncompensated solution resistance may add additional potential drops in the cell, but these will be independent of the thickness of the polymer film.

(9) Pickup, P. G.; Kutner, W.; Leidner, C. R.; Murray, R. W. *J. Am. Chem. Soc.* **1984**, *106*, 1991–1998.

(10) Ochmanska, J.; Pickup, P. G. *J. Electroanal. Chem.* **1991**, *297*, 211–224.

(11) Pickup, P. G. *J. Chem. Soc., Faraday. Trans.* **1990**, *86*, 3631–3636.

Table I. Parameters Describing Potential Profiles Across Poly-MPMP$^+$ During the Mediated Oxidation of Ferrocene[a]

current density, A cm^{-2}	E_S, V	$E_{Pt}(d = 10\ \mu m)$	s, mV
1.1	0.34	0.72	43
2.2	0.36	0.75	47
3.3	0.37	0.77	47
4.4	0.38	0.79	50
5.5	0.40	0.80	52
6.6	0.41	0.81	53

[a] All potentials are relative to SSCE and have been corrected for the uncompensated solution IR drop.

Figure 3 shows plots of potential vs film thickness for oxidation of ferrocene at a number of different current densities at rotating poly-MPMP$^+$ coated electrodes. These data were taken from the rotating disk voltammograms shown in Figure 2 (and others recorded under the same conditions). E_{Pt} is the applied potential after correction for the uncompensated solution resistance.

The plots shown in Figure 3 also represent the potential profile across a 10-μm poly-MPMP$^+$ film during oxidation of ferrocene under the same conditions. The potential exhibits a logarithmic dependence on distance across the film as shown by the least-squares fits in Figure 3. Thus, the potential profile across a poly-MPMP$^+$ film during the mediated oxidation of ferrocene can be represented by the empirical expression

$$E = E_{Pt} + s \ln (x/d) \quad (1)$$

where E_{Pt} is the potential at the polymer/electrode interface (the applied potential vs SSCE), x is distance across the film from the polymer/solution interface, d is the film thickness, and s is an empirical parameter which varies slightly with current density (Table I).

The potential at the polymer solution interface (E_s) can be determined using a bare electrode, and selected values are presented in Table I. It is clear that eq 1 becomes inaccurate close to the polymer/solution interface, since the potential here is not $-\infty$. Comparison of the E_s values in Table I with the potential profiles in Figure 3 indicates that a large fraction of the potential drop across the film occurs in a very thin section of the film at the polymer/solution interface. Thus, the empirical correlation reported here may not hold for very thin films.

Conductivity as a Function of Potential. An empirical relationship between conductivity and potential can be obtained from a simple treatment of the rotating disk data. Consider a thin layer of polymer parallel to the plane of the electrode. If this layer is sufficiently thin, the potential gradient can be taken as linear and the conductivity (σ) of this layer can be determined in the normal way:

$$\sigma = I/A(dE/dx) \quad (2)$$

From eq 1 we obtain $dE/dx = s/x$, hence

$$\sigma = Ix/sA \quad (3)$$

Equation 3 provides the conductivity profile across a film at a certain current. At the polymer/electrode interface, $x = d$ and the potential of the polymer is the applied potential, E_{Pt}. The conductivity of the polymer at this potential is therefore given by

$$\sigma(E_{Pt}) = Id/sA \quad (4)$$

This equation, which was previously derived by assuming an exponential dependence of σ on potential,[2] now has an empirical basis. It should be noted that the inaccuracy of eq 1 close to the polymer/solution interface is of little consequence here since we are analyzing the potential gradient at the polymer/electrode interface.

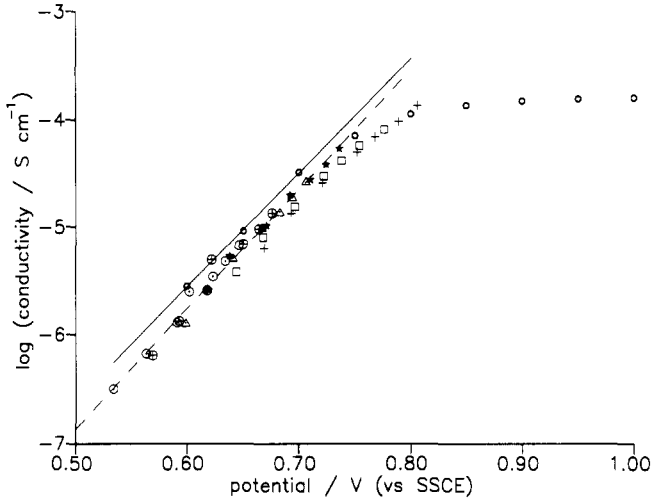

Figure 4. Conductivity vs potential for poly-MPMP$^+$ in acetonitrile + 0.1 M Et_4NBF_4, from rotating disk voltammetry (⊙, 0.5 μm; ⊕, 1 μm; Δ, 2 μm; ★, 4 μm; □, 6 μm; +, 10 μm) and from dual-electrode voltammetry (○). The solid and dashed lines are linear least-squares fits through the dual-electrode data to 0.7 V and the rotating disk data to 0.7 V, respectively.

A composite plot of conductivity vs potential derived from rotating disk voltammograms of ferrocene at poly-MPMP$^+$ films with thicknesses from 0.5 to 10 μm is shown in Figure 4. Each data set in Figure 4 was obtained from a single voltammogram like those shown in Figure 2. The conductivity at each applied potential (E_{Pt}) was calculated from the steady-state current density (I/A) by using eq 4 and the empirical value of s determined from a plot of E_{Pt} vs ln d for all films at that current density. Changes in the Donnan potential with the oxidation state of the polymer will be minimal due to the high concentration of pyridinium sites (5–6 M[7]) and so have been ignored.

Also shown in Figure 4 are conductivity vs potential data from dual-electrode voltammetry. In this experiment the potential difference across the polymer is small (10 mV), and so the potential profile can be treated as linear.[10] The conductivity of the film is measured as a function of the potential (vs SSCE) applied to the underlying Pt electrode (or the overlying Au electrode). Thus this measurement should produce results equivalent to those from rotating disk voltammetry. Each data point from dual-electrode voltammetry in Figure 4 represents an average for three poly-MPMP$^+$ films (0.25, 0.5, and 0.75 μm).

An exponential increase in conductivity with increasing potential up to ca. 0.7 V is observed with both methods. Slopes of 90 and 94 mV/decade are obtained from the rotating disk and dual-electrode data, respectively. The conductivity at 0.7 V is 2.3×10^{-5} S cm^{-1} from rotating disk voltammetry and 3.3×10^{-5} S cm^{-1} from dual-electrode voltammetry. The agreement between the two methods is very good, suggesting that the assumptions made have been reasonable.

Discussion

The results presented here confirm that nonlinear potential gradients are produced in a conducting polymer during electrolysis of a solution species. Under steady-state conditions, there is a linear increase in conductivity across the polymer film from the polymer/solution interface (eq 3), which results from a logarithmic increase in potential. Since conductivity is generally proportional to the concentration of charge carriers, it appears that electron

transport occurs across a constant concentration gradient of oxidized redox sites. Thus the conducting polymer behaves like a redox polymer in this case.[12]

Rotating disk voltammetry is an excellent method for investigating the potential-dependent conductivity of moderately conducting polymers. From the perspective of using these materials as mediators in electroanalysis or electrosynthesis, this method has the advantage that conductivity measurements can be made under conditions similar to those of the application. The new treatment presented here is more accurate at potentials close to, and above, the formal potential than our previously reported method.[2,10]

(12) Pickup, P. G.; Murray, R. W. *J. Am. Chem. Soc.* **1983**, *105*, 4510–4514.

The conductivity results presented in Figure 4 are of value in the interpretation of impedance measurements on poly-MPMP$^+$. The ionic and electronic conductivities of oxidized poly-MPMP$^+$ are very similar, and it has therefore been difficult to assign values from impedance measurements.[11] The new in situ electronic conductivities reported here indicate that fully oxidized poly-MPMP$^+$ is approximately an order of magnitude more conductive than previously reported.[2]

Acknowledgment. Financial support from the Natural Sciences and Engineering Research Council of Canada (NSERC) and Memorial University is gratefully acknowledged.

Registry No. MPMPBF$_4$, 122202-27-1; poly-MPMP$^+$, 125357-35-9; CH_3CN, 75-05-8; Et_4NBF_4, 429-06-1; Pt, 7440-06-4; ferrocene, 102-54-5.

Crystal Chemistry of Colquiriite-Type Fluorides

Yaobo Yin and Douglas A. Keszler*

Department of Chemistry and Center for Advanced Materials Research, Gilbert Hall 153, Oregon State University, Corvallis, Oregon 97331-4003

Received December 4, 1991. Revised Manuscript Received January 27, 1992

Crystal structures of six fluorides in the family LiMM′F$_6$ (M = Sr or Ca; M′ = Al, Ga, or Cr) have been refined with single-crystal X-ray diffraction data. Each compound crystallizes in trigonal space group $P\bar{3}1c$ (Z = 2) as an ordered derivative of the Li_2ZrF_6 structure type. Cell parameters: LiCaAlF$_6$, a = 5.007 (1), c = 9.641 (1) Å; LiCaGaF$_6$, a = 5.079 (3), c = 9.752 (2) Å; LiCaCrF$_6$, a = 5.098 (2), c = 9.775 (1) Å; LiSrAl$_{0.59(1)}$Cr$_{0.41(1)}$F$_6$, a = 5.117 (3), c = 10.275 (1), Å; LiSrGaF$_6$, a = 5.154 (1), c = 10.321 (2) Å; LiSrCrF$_6$, a = 5.174 (5), c = 10.369 (1) Å. Each cation occupies a deformed octahedral site in a distorted hexagonally closest-packed F$^-$ arrangement; the distortions of the D_3 M′ site are examined in detail.

Introduction

Because of their long operational lifetimes, reliable and efficient flash lamp or diode pumping, and high beam quality at high average power levels, tunable solid-state lasers can offer considerable advantages over conventional dye lasers. Recently, two new tunable laser materials, Cr^{3+}:LiCaAlF$_6$ and Cr^{3+}:LiSrAlF$_6$, were reported.[1,2] These materials exhibit high intrinsic lasing efficiency, low thermal lensing, and excellent resistance to UV solarization. Each host, however, exhibits unique lasing and optical characteristics. For example, the Ca derivative exhibits a higher intrinsic efficiency of 67% vs 53% for the Sr derivative, a smaller π emission cross section of 1.3×10^{-20} cm^2 vs 4.8×10^{-20} cm^2, and a longer emission lifetime of 170 μs vs 67 μs. These characteristics are determined by the static and dynamic characteristics of the hosts and, in particular, the characteristics of the Al dopant site. In a recent account we described the static distortions of the AlF$_6$ site in the host LiSrAlF$_6$ that contribute to the heightened cross section and shorter lifetime of the Cr^{3+} optical emission.[3]

In this report we present crystal data on colquiriite (LiCaAlF$_6$)[4] and its derivatives LiCaCrF$_6$, LiCaGaF$_6$, LiSrAl$_{0.59(1)}$Cr$_{0.41(1)}$F$_6$, LiSrCrF$_6$, and LiSrGaF$_6$, some of which are being developed as new laser materials.

* To whom correspondence should be addressed.

Experimental Section

The single crystals of LiCaCrF$_6$, LiSrGaF$_6$, LiCaAlF$_6$, and LiSrAl$_{0.59}$Cr$_{0.41}$F$_6$ were grown at Lawrence Livermore National Laboratory, and the single crystals of LiCaGaF$_6$ and LiSrCrF$_6$ were prepared at Oregon State University. Reagents used for crystal growth at OSU were the following: LiF (AESAR, 99.99%), CaO (AESAR, 99.95%), Ga_2O_3 (AESAR, 99.999%), SrF_2 (Cerac, 99%), and Cr_2O_3 (Johnson Matthey, 99%). A powder of LiCaGaF$_6$ was prepared by passing HF(g) (Matheson, 99.9%) over a stoichiometric mixture of the starting reagents at 700 °C for 1 h followed by annealing at the same temperature for 12 h. The single crystal was grown by maintaining the melt at 850 °C for 20 min and then rapidly cooling to and annealing at 700 °C for 24 h. A colorless single crystal of dimensions 0.1 × 0.1 × 0.1 mm was physically separated from the solidified melt. The single crystal of LiSrCrF$_6$ having dimensions 0.1 × 0.08 × 0.1 mm was obtained by passing HF(g) over the mixture SrF_2:1.5LiF:0.75Cr_2O_3 at 650 °C for 2 h and then heating to 810 °C and cooling to 700 °C at a rate of 12 °C/h.

The single crystals were mounted on glass fibers and analyzed on a Rigaku AFC6R diffractometer. Cell parameters were obtained from least-squares refinement of the setting angles of 10–19

(1) Payne, S. A.; Chase, L. L.; Newkirk, H. W.; Smith, L. K.; Krupke, W. F. *IEEE J. Quantum Electron.* **1988**, *24*, 2243.
(2) Payne, S. A.; Chase, L. L.; Smith, L. K.; Kway, W. L.; Newkirk, H. W. *J. Appl. Phys.* **1989**, *66*, 1051.
(3) Schaffers, K. I.; Keszler, D. A. *Acta Crystallogr., Sect. C* **1991**, *47*, 18.
(4) Viebahn, V. W. *Z. Anorg. Allg. Chem.* **1971**, *386*, 335.

0897-4756/92/2804-0645$03.00/0